Journal of Alloys and Compounds 676 (2016) 187–192

Contents lists available at ScienceDirect

Journal of Alloys and Compounds

journal homepage: http://www.elsevier.com/locate/jalcom

Metastable Co_3C nanocrystalline powder produced via reactive ball milling: Synthesis and magnetic properties

Z. Turgut [a], M.S. Lucas [a, *], S. Leontsev [a, b], S.L. Semiatin [a], J. Horwath [a]

[a] Air Force Research Laboratory, Wright-Patterson AFB, OH 45433, USA
[b] University of Dayton Research Institute, Dayton, OH 45469-0170, USA

ARTICLE INFO

Article history:
Received 9 December 2015
Received in revised form
5 February 2016
Accepted 13 March 2016
Available online 16 March 2016

Keywords:
Hard magnets
Mechanical alloying
Coercivity
Nanocrystalline alloys
Metastable phases

ABSTRACT

This study investigates reactive ball milling synthesis of a single phase metastable Co_3C compound from starting mixtures of cobalt and graphite powders under argon and nitrogen environments. It reports their phase formations, magnetic, and structural properties. Regardless of the starting powder composition (25.0 or 33.3 at.% C) and milling atmosphere, reactive ball milling leads to the formation of the Co_3C compound with an orthorhombic structure. Coercivities of the starting mixtures first increases with milling time as the Co_3C compound starts to form and subsequently decreases due to structural defects induced by further milling. Higher graphite containing starting powder mixtures yield higher peak coercivity values and higher transformation rates. The formed Co_3C compound exhibits a Curie temperature of 563 K and a decomposition temperature around 710 K. Compared to argon milled powders, reactive milling under a nitrogen atmosphere increases the coercivity and decomposition temperature of the Co_3C compound.

1. Introduction

Two technologically important rare earth based permanent magnetic systems are NdFeB and SmCo. The NdFeB system offers higher energy products, $(BH)_{max}$ than that of the SmCo system and dominates commercial markets in both sintered and bonded magnet forms. SmCo magnets on the other hand, are the material of choice for many aerospace and military applications because of their higher operating temperatures. Ever increasing demand for high energy permanent magnets mainly due to green/renewable energy technologies coupled with high cost and the somewhat strategic nature of the rare earth elements has sparked an interest in developing rare earth free/lean permanent magnet systems. It seems highly unlikely that a cheaper rare earth free alternative with energy products comparable to those of the rare earth based magnets will be developed in the near future. It is easy however to predict that a substantially cheaper rare earth free alternative, with moderate energy densities, would capture a large share of the permanent magnet market and ease the demand on rare earths.

On rare earth lean front, efforts to synthesize exchange spring coupled nanocomposite magnets that were first suggested by Kneller and Hawig [1] still continues mainly on the Sm–Co system [2–4]. On rare earth free front, a handful of candidate systems all previously known to the scientific community are being revisited. Among these are Zr_2 Co_{11} [5], FeNi [6], AlNiCo [7], $HfCo_7$ [8], MnBi [9] and MnAlC [10]. The Co–C system is one of these alloy groups that have recently been studied as a rare earth free permanent magnetic system.

There are no stable compounds of Co–C, however metastable Co_3C or Co_2C , mostly in a mixed form, can be stabilized by non-equilibrium synthesis techniques such as ball-milling [11,12], Kratschmer carbon arc process [13], wet chemical synthesis [14–17] and pulse laser ablation [18] techniques. Both Co_3C and Co_2C form into an orthorhombic structure with space groups P_{bnm} and P_{nnm} respectively [11]. Chemical synthesis yields nanocrystalline Co_3C and Co_2C phase mixtures with moderate properties; H_C = 271 kA/m (3.4 kOe), T_C = 613 K, $(BH)_{max}$ = 20 kJ m^{-3} (2.51 MGOe). Decomposition temperatures of these phase mixtures range from 700 to 797 K. It is important to note that these properties were determined for free standing nanopowders, where the coercivity could have a large component that is due to surface anisotropy rather than magnetocrystalline anisotropy. Indeed Zhang et al. [15] reports a strong particle size dependence of coercivity in chemically synthesized powders; coercivity varies

* Corresponding author.
E-mail address: matthew.steven.lucas@gmail.com (M.S. Lucas).

http://dx.doi.org/10.1016/j.jallcom.2016.03.095
0925-8388/

from 48 kA/m (0.6 kOe) for 1000 nm size particles to 247 kA/m (3.1 kOe) for 20 nm size particles.

Previous ball milling studies of the Co–C system did not report any magnetic properties [11]. In this study, we have undertaken reactive ball milling of this system under argon and nitrogen atmospheres in order to explore its phase formations, magnetic properties, and to determine if Co_3C can be synthesized in a single phase form. Nitrogen gas was introduced to study the effect of nitrogen on the magnetic properties. Interstitial nitrogen is known to enhance Curie temperature and saturation magnetization in various magnetic systems. The ball milling process produces nanograined powder with a larger particle/agglomerate size, which should both reduce surface anisotropy effects and provide a precursor for creating bulk magnets via standard consolidation practices.

2. Experimental

Starting mixtures of cobalt (1.6 μm) and graphite (1.0 μm) powders with nominal compositions of Co-33.3 at. % C and Co-25.0 at. % C were ball milled in the presence of nitrogen and argon gases up to 20 h using a SPEX 8000 high energy ball mill. The same ball to powder ratio was used throughout the experiments to maintain constant impact strength. Starting powder to ball weight ratio was one to four. The milling process was interrupted periodically for cooling and sample collection purposes. A positive gas pressure of 34 kpa (5 psi) was introduced before the vials were sealed for milling and the same gas pressure was reconstituted after each sample collection routine. A Lake Shore vibrating sample magnetometer (VSM) equipped with a high temperature furnace was used for magnetization measurements. DSC measurements were carried out using a Perkin Elmer 8500 calorimeter. Room temperature X-ray diffraction, (XRD) measurements were carried out using a Rigaku diffractometer with a Cu–Kα source. Reitveld refinement was employed to estimate crystal lattice parameters and unit cell volume. Scanning electron microscopy (SEM) was utilized to determine particle size.

3. Results and discussion

3.1. Phase evolution during ball milling

Fig. 1 shows XRD plots of argon milled Co-33.3 at. % C starting powder composition for the milling times indicated on the graph. The starting Co powder was in the hcp structure as it is the stable form of Cobalt at room temperature; a small amount of fcc-Co was also detected. In the initial stages of the milling process, the Co + graphite mixture converts to an fcc-Co_{1-x} C_x solid solution before any carbide formation takes place. The 4 h milled samples exhibits only fcc solid solution. When milling time was extended to 8 h and beyond, all the fcc solid solution transforms to the Co_3C with an orthorhombic structure. XRD measurements on nitrogen milled powders of the same composition as well as nitrogen and argon milled powders of the Co-25.0 at. % C composition yields very similar results (Fig. 2). Formation of Co_2C was not observed.

Evolution of the phases during ball milling was also monitored by thermomagnetic $M(T)$ and DSC measurements. Fig. 3 depicts $M(T)$ curves of the nitrogen milled Co-33.3 at. % C composition with magnetization values normalized by the moment measured at room temperature. For the eight, twelve and 17 h milled samples, the drop in magnetization with increasing temperature is due to ferromagnetic to paramagnetic transformation of the Co_3C phase and the subsequent increase in magnetization is due to decomposition of it. The amount of transformed Co_3C increases with increasing milling time as indicated by the magnitude of

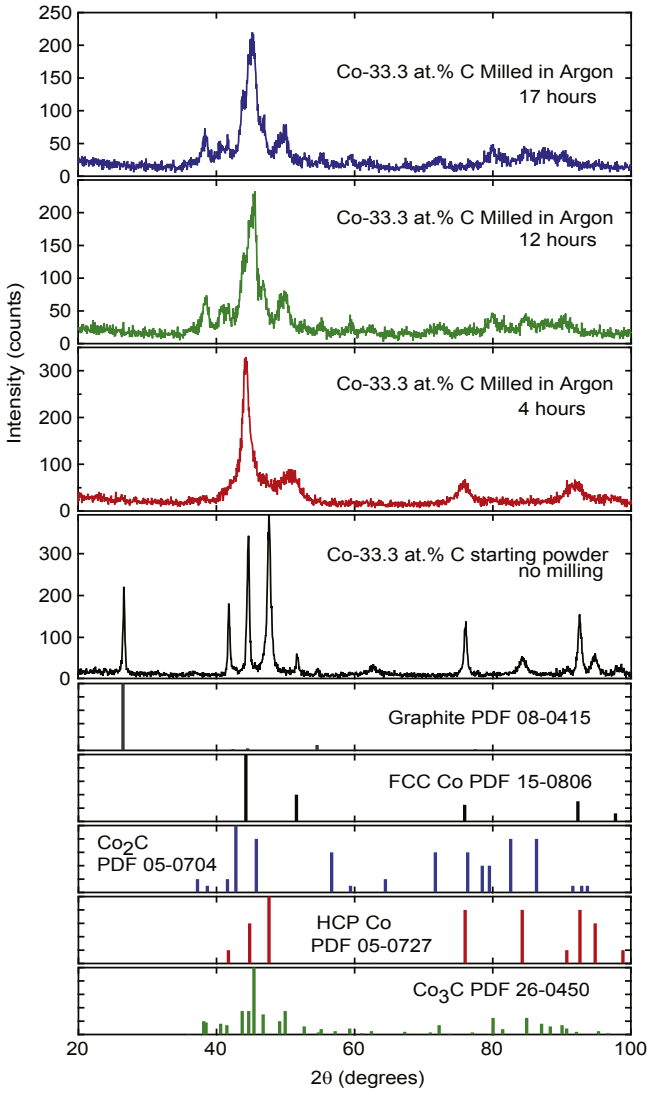

Fig. 1. XRD plots of argon milled Co-33.3 at. % C composition showing the progression with milling time. Relevant reference patterns are shown.

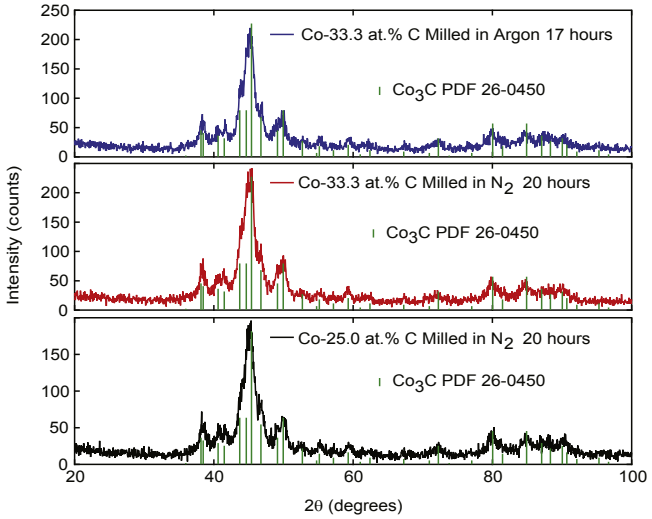

Fig. 2. XRD plots of the samples with the longest milling time. The reference pattern for Co_3C is also shown.

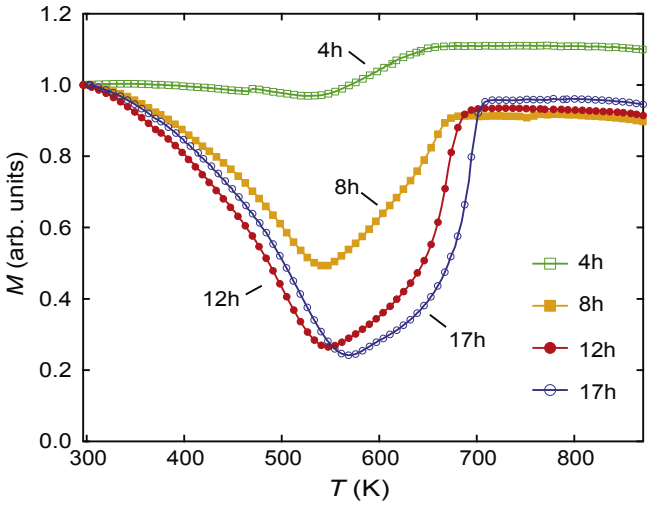

Fig. 3. Thermomagnetic $M(T)$ curves of the Co-33.3 at. % C composition prepared in N_2 for the given milling times in hours. The measurements were taken at 500 Oe (0.05 T, 39.8 kA/m).

magnetization drop at its Curie temperature. Prolonged milling times also causes an increase in decomposition temperature of the Co_3C compound. The Curie temperatures decrease as the Co_3C gets more refined with further milling up to 12 h, but then increases for the 17 h sample just as the H_C goes down. In agreement with the XRD data, 4-h milled powders did not show presence of any Co_3C ; the increase in magnetization around 548 K is most likely due to dissolution of fcc-$Co_{1-x}C_x$ and re-formation of hcp-Co.

Previous studies [19] show that extensive milling of hcp-Co leads to an hcp→fcc transformation in which the fcc phase is stabilized mainly by stacking faults introduced during the milling. In the Co–C system, stabilization of the fcc phase by defects is also believed to be an effective mechanism. The presence of C on the other hand can only increase this transformation since graphite shows solubility only in fcc-Co but not in hcp-Co, according to the Co–C equilibrium phase diagram [11].

Regardless of the starting powder composition, milling time and atmosphere, mechanical milling of Co–C mixtures led to the formation of Co_3C phase only. Lack of Co_2C formation in ball milled samples is puzzling. Various techniques listed in the introduction section, not including the ball milling synthesis, report formation of Co_2C along with Co_3C. Unlike ball milling, these synthesis routes are less invasive in terms of introduced defects. Portnoi et al. [11] reports formation of Co_2C when a supersaturated fcc phase is heated up to 823 K while the very same precursor forms Co_3C when heated to only 583 K. Iskhakov et al. [20] also reports formation of Co_2C by a pulsed plasma vaporization technique when the substrate temperature is set to 423 K; a 323 K substrate temperature however results only in formation of Co_3C. These observations may suggest a close correlation between higher defect densities and the lack of Co_2C phase formation in ball milled Co–C. Extended studies are necessary to determine the nature of the mechanisms preventing the formation of Co_2C in this non-equilibrium system.

3.2. Magnetic properties

Table 1 lists the obtained values of H_C and M_S for the studied compositions at different milling atmospheres as a function of milling time. After 4 h of milling, the fcc solid solution, whether formed under argon or nitrogen, exhibits coercivity values of 16–20 kA/m. These values are typical for magnetically soft fine particles with cubic symmetry. They usually derive their magnetic hardness from surface anisotropy and being in a single domain regime. With increasing milling time formation of the Co_3C takes place, and coercivity values start to increase as saturation magnetization decreases. A peak value in coercivity is obtained after 12 h of milling for both the argon and nitrogen milled Co-33.3 at.% C compositions. The peak value in coercivity occurs after 17 h of milling for the nitrogen milled Co-25.0 at.% C composition clearly indicating the effect of higher carbon content on transformation rate. The amount of transformed volume as well as the presence of nitrogen had a noticeable effect on coercivity values. After the peak in coercivity, the reduction is believed to be due to a reduction in crystallinity due to defects induced by the ball milling process.

The primary property of a permanent magnet is its coercivity which in many cases has its origins in magnetocrystalline anisotropy. At moderately high fields where all possible wall displacement has taken place and a ferromagnet is close to its saturation, the experimental data can be fit into the law of approach to saturation (LAS) in order to estimate the magnetic anisotropy constant, K. The LAS is written as [21,22];

$$M = M_S\left(1 - \frac{b}{H^2}\right) + \chi_\circ H \tag{1}$$

Where;

$$b = \frac{4}{15}\frac{K^2}{M_S^2} \tag{2}$$

In this expression M_S is the spontaneous magnetization and $\chi_\circ$ is the high field susceptibility. The specific magnetization values were estimated using a calculated density value for Co_3C. By curve-fitting the above equations to the experimental data, the K values of the nitrogen milled Co-33.3 at. % C composition were calculated and given in Fig. 4 as a function of milling time, along with the anisotropy field, Ha, which is estimated by using $Ha=2K/M_S$. The values obtained from this analysis do not necessarily represent the anisotropy constant and anisotropy field of the Co_3C (these values are usually measured on single crystals and are intrinsic in nature). They are instead used to illustrate the dynamic nature of the ball milling process. The decreasing trend in K and H_a (Fig. 4) with increasing milling time is a clear evidence of the defect inducing nature of the ball milling process.

In a dry milling process, powder particles are subjected to repeated fracture and cold welding due to highly energetic compressive impacts of the milling media. This process leads to a diminished crystallinity and associated reduction in anisotropy constant with increasing milling time and consequently leads to reduced coercivity values. An extreme example for this effect would be the magnetically soft nature of permanent magnetic systems in amorphous form [23]. Despite the reduced anisotropy constant with increasing milling time, the initial increase trend in coercivity as a function of milling time is mainly attributed to a reduction in particle size and defects introduced during milling. Coercivity of any ferromagnetic system goes through a maximum as a function of reduced grain or particle diameter. The peak in coercivity is observed when the grain or particulate size gets closer towards a value called exchange length (L_{ex}), where it is no longer energetically favorable for the particles to possess multi-domains. For larger particulate sizes, where material exhibit a multi-domain behavior, structural defects introduced during ball milling cause an increase in coercivity by hindering domain wall motion. Once the material is milled beyond the single domain limit, the reduction in coercivity is usually attributed to a thermally activated switching process [24]. It is these competing mechanisms of size

Table 1
Evolution of coercivity and saturation magnetization as a function of milling time.

Milling time (hours)	Co-33.3 at. % C (Argon milled)		Co-33.3 at. % C (Nitrogen milled)		Co-25.0 at. % C (Nitrogen milled)	
	H_c (kA/m)	M_s (emu/g)	H_C (kA/m)	M_s (emu/g)	H_C (kA/m)	M_s (emu/g)
4	17.0	121.6	20.4	108.9	16.4	122.8
8	44.7	89.6	68.2	71.9	45.9	78.7
12	78.3	68.7	100.7	59.2	55.9	71.9
17	65.2	68.1	80.4	59.4	64.1	64.7
20	–	–	74.1	62.1	62.6	64.2

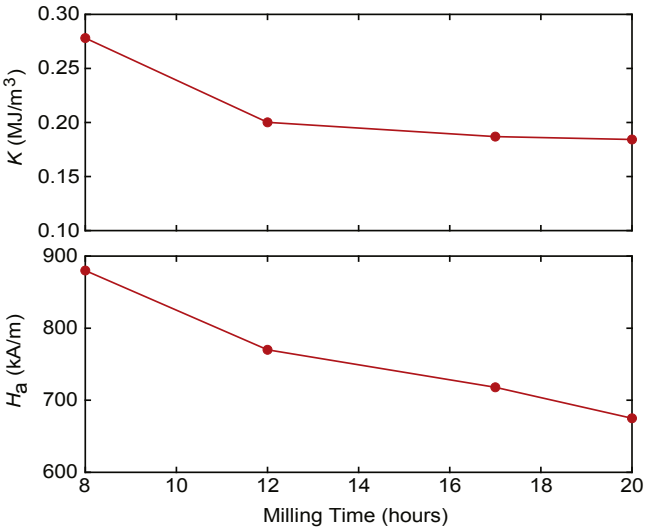

Fig. 4. Calculated K and H_a values as a function of milling time for nitrogen milled Co-33.3 at.% C composition.

reduction, increased defect density, and reduced crystallinity that determine the observed trend in coercivity with milling time.

In order to provide further support for the above argument, 12 and 17 h nitrogen milled Co-33.3 at.% C samples were subjected to a low temperature annealing at 473 K up to 12 h. The annealing temperature was chosen to be low enough so that no grain growth could occur but high enough to provide enough driving force for atomic diffusion to eliminate structural defects. As depicted in Fig. 5, coercivity increases for both samples with annealing. The increase in coercivity, ΔH_c being the difference between as milled and annealed coercivity values, was greater for the 17 h milled sample which is expected to have higher defect densities.

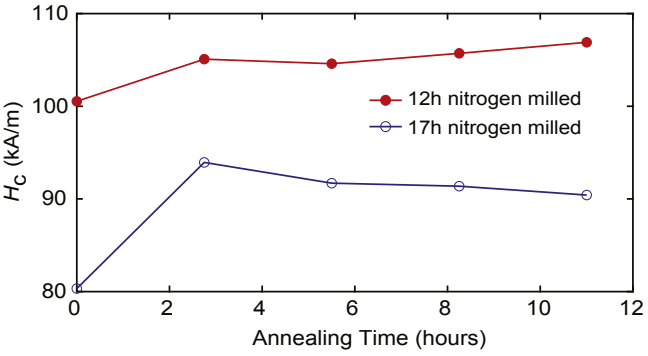

Fig. 5. Effect of 473 K annealing on coercivity for nitrogen milled Co-33.3 at.% C compositions.

Coercivity of the 17 h milled samples also plateaued a lot faster than the 12 h milled sample as higher defect densities should promote higher diffusion rates.

Measured coercivity values of our milled materials were lower than that of polyol processed powders; Harris et al. [14] reported a room temperature coercivity value of ≈ 246.7 kA/m (3.1 kOe) for their $Co_2C + Co_3C$ phase mixtures. Zhang et al. [15] also reported similar values for 20 nm $Co_2C + Co_3C$ mixtures while coercivity dropped to 135 and 48 kA/m for 200 and 1000 nm nanoparticles respectively. SEM analysis of our ball milled powders showed clumps of irregularly shaped 200–350 nm size particles (Fig. 6); Scherrer analysis on the other hand indicated an average grain size of ~ 22 nm for 20 h milled powders. The observed coercivity values in this study agree well with the results of Zhang et al. Saturation

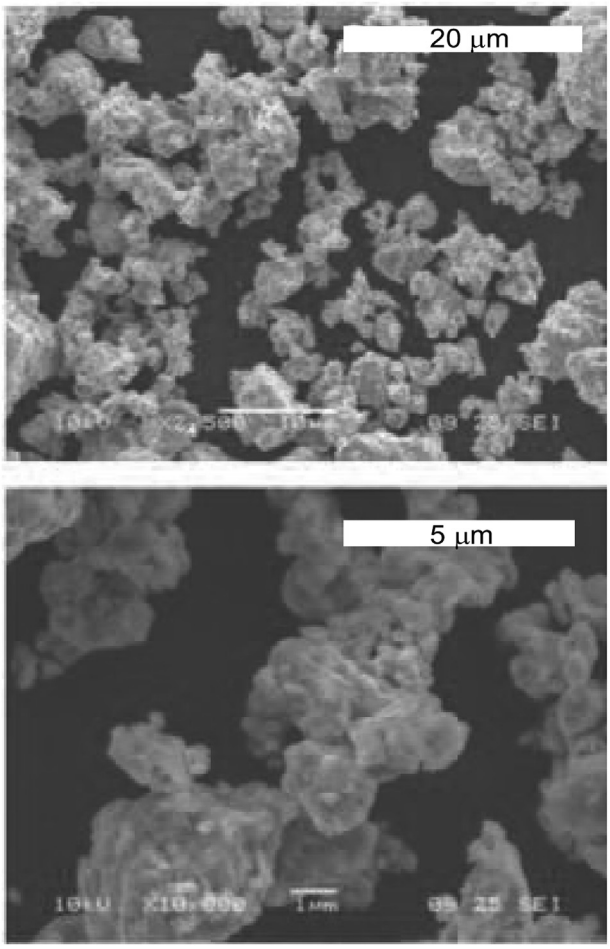

Fig. 6. Overall particle morphology of 17 h milled Co-33.3 at. % C composition.

magnetizations of ~ 59–68 emu/g exhibited by our powders were higher than those reported for polyol processed powders. The difference is an apparent result of single Co_3C phase of this study versus $Co_2C + Co_3C$ phase mixtures obtained by polyol processing. Huba et al. [16] was able to chemically synthesize single phase Co_2C nanoparticles with an M_S value of 16 emu/g which is lower than that of Co_3C.

3.3. Effect of nitrogen

Partly inspired by the positive effects of dissolved nitrogen in ferromagnetic systems, nitrogen gas was introduced as a milling atmosphere. Nitrogen is known to enhance magnetic properties of certain rare earth based permanent magnet systems [25,26] and help stabilize $L1_0$ phase in FePt alloys [27] (there is an excellent review by Coey and Smith [28] on the effect of nitrogen in ferromagnetic systems). No attempt was made to quantify the amount of nitrogen going into the solid solution but it was obvious from negative pressures forming in nitrogen filled vials during milling that nitrogen was reacting with the powder mixture. No such negative pressure formation was observed in argon filled vials. As shown in Fig. 7a, the presence of nitrogen increases coercivity compared to the argon milled samples. Another obvious effect of nitrogen is increased transformation rates. Fig. 7b compares thermomagnetic curves of 12 h argon and nitrogen milled powders. Since the magnitude of the magnetization drop at the T_C of the Co_3C compound is directly correlated to the amount of it, nitrogen is highly effective in increasing the transformation rate. The effect of nitrogen on T_C of the Co_3C however was not so obvious since it strongly depends on milling time and resulting transformed volume. DSC measurements (Fig. 8) reveal a decomposition temperature of 687 K for the 12 h nitrogen milled powder while 12 h argon milled powder of the same composition decomposes at 657 K. The highest decomposition temperature of 710 K was measured on 20 h

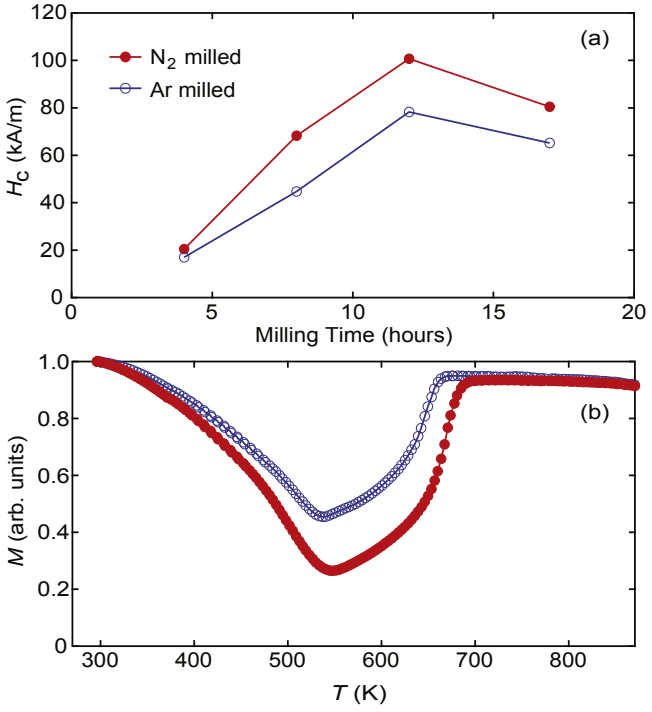

Fig. 7. Evolution of coercivity with milling time (a) and thermomagnetic plots of 12 h milled Co-33.3 at. % C composition (b) for the two different milling environments.

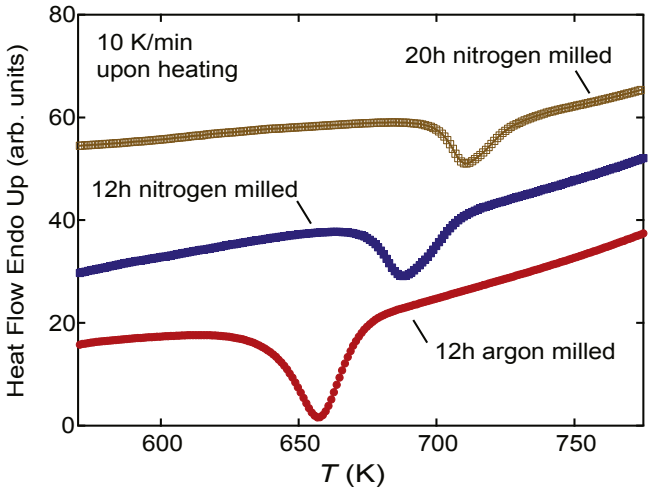

Fig. 8. DSC plots of Co-33.3 at.% C composition for indicated milling time and environments.

nitrogen milled Co-25.0 at.% C sample.

Fig. 9 shows the results of Rietveld analysis of the XRD patterns plotted against the milling time. At low milling times the nitrogen milled samples exhibit smaller unit cell volumes compared to the argon milled samples (Fig. 9a). This is a clear indication of nitrogen, with its smaller atomic volume compared to carbon, reacting with the material and actively participating in the formation of the orthorhombic structure. By contrast, there should be no reaction to the inert gas in the argon milled samples. Such difference in atomic volume coupled with the difference in valences of nitrogen and carbon may also explain the beneficial effects of nitrogen on

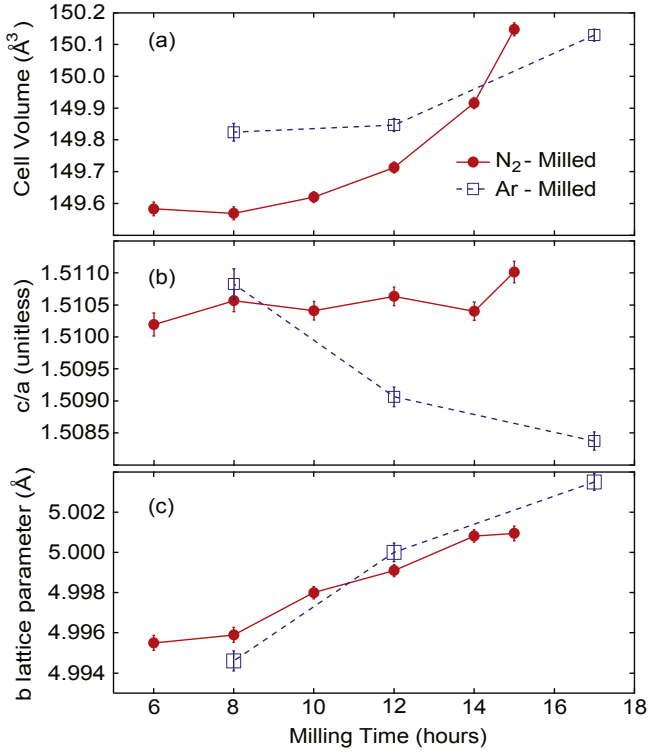

Fig. 9. Change of (a) unit cell volume, (b) c/a ratio, and (c) the b lattice parameter as a function of milling time for Co-33.3 at. % C composition in argon and nitrogen.

transformation rate. With prolonged milling times of 14 h and beyond, the unit cell volume of nitrogen milled powders becomes comparable to that of argon milled samples. This is ascribed to changing a and c parameters with increasing milling time (Fig. 9b); the b lattice parameter of the argon and nitrogen milled powders (Fig. 9c) are comparable and increase almost linearly with time for both milling environments. The improved coercivity values in the nitrogen milled samples could be due to the corresponding enhancement of the c/a ratio compared to argon milled powders. Although it is not universal, lowered crystalline symmetry often improves the magnetic anisotropy energy and the coercivity [29–32].

3.4. Iron contamination during milling

A fully formed Co_3C material is expected to exhibit paramagnetic behavior between its Curie and decomposition temperatures. Despite the milling times up to 20 h however, a residual magnetization existed at temperatures above the T_C of Co_3C indicating the presence of a ferromagnetic phase. At first glance, this residual magnetization may seem to be the result of some untransformed $Co_{1-x}C_x$ solid solution but results of the thermomagnetic measurements taken up to 1273 K convinced us that this non-vanishing magnetization behavior is most likely due to iron contamination from steel milling vials and balls employed in this study. Similar contamination issues were reported for ball milled Co powders [33,34]. Fig. 10 shows the thermomagnetic curve of Co-25.0 at.% C composition that was milled in nitrogen atmosphere for 20 h. The presence of Fe is evident from the magnetization drop at a temperature where T_C of Fe is expected to occur (T_C of iron ~ 1041 K). The magnitude of the residual magnetization corresponds well to the magnitude of magnetization drop at the Curie temperature of iron. None of the demagnetization curves showed a two phase behavior which is usually characterized by a step in demagnetizations curves, indicating that free Fe is magnetically coupled to the Co_3C matrix.

4. Summary and conclusions

Reactive ball milling of Co–C has been used to synthesize metastable Co_3C as a single phase with an orthorhombic structure. The transformation follows hcp-Co + C → fcc-$Co_{1-x}C_x$ → Co_3C route. Co_2C does not form under the conditions employed in this study. Dissolved nitrogen is found to be an effective agent in increasing transformation rate, coercivity, and decomposition temperature of Co_3C. A fully formed Co_3C exhibits an M_S value of 60–62 emu/g, a Curie temperature of ≈ 563 K and decomposes around 710 K.

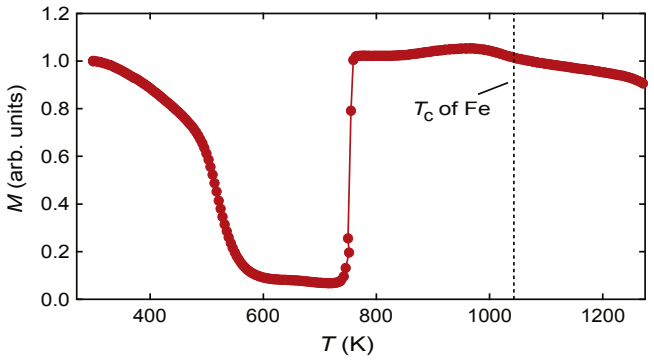

Fig. 10. Thermomagnetic $M(T)$ plot of 20 h nitrogen milled Co-25.0 at.% C composition. The measurement was taken at 500 Oe (0.05 T, 39.8 kA/m). The Curie temperature of Fe is given by the vertical dashed line.

Compared to polyol processed powders that have smaller particle size and are in freestanding form, ball milled Co_3C material exhibits lower coercivity values of 106 kA/m (1.34 kOe, the maximum coercivity obtained in 473 K annealed samples). There are ways such as cryo-milling or surfactant assisted ball milling to bring the particle size of ball milled powders close to those of polyol processed powders and increase coercivity. If coercivity values of over 240 kA/m (3 kOe) can be retained in consolidated materials, Co_3C can be a potential candidate as a permanent magnet with energy products comparable to those of Alnico and magnetically hard ferrites.

Acknowledgments

This work is partially supported by a grant from the US Air Force Office of Scientific Research (AFOSR).

References

[1] E.F. Kneller, R. Hawig, IEEE Trans. Magnetics 27 (1991) 3588.
[2] Y. Shen, M.Q. Huang, Z. Turgut, M.S. Lucas, E. Michel, J.C. Horwath, J. Appl. Phys. 111 (2012) 07B512.
[3] S.K. Pal, L. Schultz, O. Gutfleisch, J. Appl. Phys. 113 (2013) 013913.
[4] C. Rong, Y. Zhang, N. Poudyal, D. Wang, M.J. Kramer, J.P. Liu, J. Appl. Phys. 109 (2011) 07A735.
[5] W. Zhang, S.R. Valloppilly, R.S.X. Li, J.E. Shield, D.J. Sellmyer, IEEE Trans. Magn. 48 (2012) 3603.
[6] L.H. Lewis, A. Mubarok, E. Poirier, N. Bordeaux, P. Manchanda, A. Kashyap, R. Skomski, J. Goldstein, F.E. Pinkerton, R.K. Mishra, R.C. K Jr., K. Barmak, J. Phys. Condens. Matter 26 (2014) 064213.
[7] Q. Xing, M.K. Miller, L. Zhou, H.M. Dillon, R.W. McCallum, I.E. Anderson, S. Constantinides, M.J. Kramer, IEEE Trans. Magn. 49 (7) (2013) 3314.
[8] B. Balamurugan, B. Das, V.R. Shah, R. Skomski, X.Z. Li, D.J. Sellmyer, Appl. Phys. Lett. 101 (2012) 122407.
[9] Y.Q. Li, M. Yue, J.H. Zuo, D.T. Zhang, W. Liu, J.X. Zhang, Z.H. Guo, W. Li, IEEE Trans. Magn. 49 (7) (2013) 3391.
[10] O. Kohmoto, N. Kageyama, Y. Kageyama, H. Haji, M. Uchida, Y. Matsushima, J. Phys. Conf. Ser. 266 (2011) 012016.
[11] V.K. Portnoi, A.V. Leonov, Inorg. Mater. 48 (6) (2012) 593.
[12] L.D. Barriga-Arceo, E. Orozco, V. Garibay-Febles, L. Bucio-Galindo, P.C.-O.H. Mendoza León, A. Montoya, J. Phys. Condens. Matter 16 (2004) S2273.
[13] M.E. McHenry, S.A. Majetich, J.O. Artman, M. DeGraef, S.W. Staley, Phys. Rev. B 49 (1994) 11358–11363.
[14] V.G. Harris, Y. Chen, A. Yang, S. Yoon, Z. Chen, A.L. Geiler, J. Gao, C.N. Chinnasamy, L.H. Lewis, C. Vittoria, E.E. Carpenter, K.J. Carroll, R. Goswami, M.A. Willard, L. Kurihara, M. Gjoka, O. Kalogirou, J. Phys. D Appl. Phys. 43 (16) (2010) 165003.
[15] Y. Zhang, G.S. Chaubey, C. Rong, Y. Ding, N. Poudyal, P. ching Tsai, Q. Zhang, J.P. Liu, J. Magnetism Magnetic Mater. 323 (2011) 1495–1500.
[16] Z.J. Huba, E.E. Carpenter, J. Appl. Phys. 111 (2012) 07B529.
[17] K.J. Carroll, Z.J. Huba, S.R. Spurgeon, M. Qian, S.N. Khanna, D.M. Hudgins, M.L. Taheri, E.E. Carpenter, Appl. Phys. Lett. 101 (2012) 012409.
[18] S.H. Huh, A. Nakajima, J. Appl. Phys. 99 (6) (2006) 064302.
[19] J.Y. Huang, Y.K. Wu, H.Q. Ye, Appl. Phys. Lett. 66 (3) (1995) 308–310.
[20] R. Iskhakov, S. Stolyar, L. Chekanova, E. Artem'ev, V. Zhigalov, J. Exp. Theor. Phys. Lett. 72 (6) (2000) 316–319.
[21] S. Chikazumi, Physics of Ferromagnetism, Oxford Univ. Press Inc., New York, 1997.
[22] G. Hadjipanayis, D.J. Sellmyer, B. Brandt, Phys. Rev. B 23 (1981) 3349–3354.
[23] A. Inoue, A. Takeuchi, A. Makino, T. Masumoto, IEEE Trans. Magn. 31 (1995) 3626–3628.
[24] E.F. Kneller, F.E. Luborsky, J. Appl. Phys. 34 (3) (1963) 656–658.
[25] J. Coey, H. Sun, D. Hurley, J. Magnetism Magnetic Mater. 101 (1991) 310.
[26] T. Iriyama, K. Kobayashi, N. Imaoka, T. Fukuda, H. Kato, Y. Nakagawa, IEEE Trans. Magn. 28 (1992) 2326.
[27] O. Dmitrieva, M. Acet, G. Dumpich, J. Kästner, C. Antoniak, M. Farle, K. Fauth, J. Phys. D Appl. Phys. 39 (2006) 4741.
[28] J. Coey, P. Smith, J. Magnetism Magnetic Mater. 200 (1999) 405.
[29] T. Burkert, L. Nordström, O. Eriksson, O. Heinonen, Phys. Rev. Lett. 93 (2004) 027203.
[30] A. Asali, P. Tonson, P. Blaha, J. Fidler, IEEE Trans. Magn. 50 (11) (2014) 7027504.
[31] S. Kauffmann-Weiss, S. Hamann, M.E. Gruner, L. Schultz, A. Ludwig, S. Fähler, Acta Mater. 60 (2012) 6920.
[32] O. Hjortstam, K. Baberschke, J.M. Wills, B. Johansson, O. Eriksson, Phys. Rev. B 55 (1997) 15026.
[33] F. Cardellini, G. Mazzone, Philos. Mag. A 67 (1993) 1289.
[34] J.Y. Huang, Y.K. Wu, H.Q. Ye, Appl. Phys. Lett. 67 (1995) 1945.